Published in final edited form as:
*Cell Mol Bioeng*. 2012 September 1; 5(3): 327–336. doi:10.1007/s12195-012-0240-0.

# Cardiogenic Regulation of Stem-Cell Electrical Properties in a Laser-Patterned Biochip

**Zhen Ma**[1], **Qiuying Liu**[1,2], **Honghai Liu**[1], **Huaxiao Yang**[1], **Julie X. Yun**[1], **Meifeng Xu**[3], **Carol A. Eisenberg**[4], **Thomas K. Borg**[5], **Roger Markwald**[5], and **Bruce Z. Gao**[1,#]

[1]Department of Bioengineering, COMSET, Clemson University, Clemson, South Carolina, USA

[2]Biomedical R&D Center, Jinan University, Guangzhou, P. R. China

[3]Department of Pathology and Laboratory Medicine, University of Cincinnati Medical Center, Cincinnati, Ohio, USA

[4]New York Medical College/Westchester Medical Center Stem Cell Laboratory, New York Medical College, Valhalla, New York, USA

[5]Department of Regenerative Medicine and Cell Biology, Medical University of South Carolina, Charleston, South Carolina, USA

## Abstract

Normal cardiomyocytes are highly dependent on the functional expression of ion channels to form action potentials and electrical coupling with other cells. To fully determine the scientific and therapeutic potential of stem cells for cardiovascular-disease treatment, it is necessary to assess comprehensively the regulation of stem-cell electrical properties during stem cell-cardiomyocyte interaction. It has been reported in the literature that contact with native cardiomyocytes induced and regulated stem-cell cardiogenic differentiation. However, in conventional cell-culture models, the importance of cell-cell contact for stem-cell functional coupling with cardiomyocytes has not been elucidated due to insufficient control of the cell-contact mode of individual cells. Using microfabrication and laser-guided cell micropatterning techniques, we created two biochips with contact-promotive and -preventive microenvironments to systematically study the effect of contact on cardiogenic regulation of stem-cell electrical properties. In contact-promotive biochips, connexin 43 expression was upregulated and relocated to the junction area between one stem cell and one cardiomyocyte. Only stem cells in contact with cardiomyocytes were induced by adjacent cardiomyocytes to acquire electrophysiological properties for action-potential formation similar to that of a cardiomyocyte.

### Keywords

Microenvironment; Laser guidance; Biochip; Electrical coupling; Cell contact

## Introduction

Identifying in vitro cell responses to stimuli from neighboring cells provides knowledge vital to understanding higher-level organization of tissues and organs. This understanding is essential for using regenerative medicine-based therapeutic approaches to reconstruct damaged tissues, such as an infarcted myocardium. One example of such a therapeutic

[#]Corresponding author: Bruce Z. Gao, Ph.D., Address: 201-5 Rhodes Hall, Department of Bioengineering, Clemson University, Clemson, South Carolina, 29634, USA, Tel: (864) 656-0185, zgao@clemson.edu.

approach is to use stem cells for myocardial regeneration, which has been the subject of research for 20 years[1]. Key issues in this study are to determine whether stem cells can be functionally coupled with native cardiac cells and whether these couplings require cardiogenic regulation of stem-cell properties. Stem-cell coupling with cardiac cells is intimately affected by the cellular microenvironment, which exerts chemical and physical stimulating factors.

To decipher the effects of cell-microenvironment interactions on functional cell couplings, stem cells have been cultured and compared under two conditions: (1) culturing stem cells with cardiomyocyte-conditioned medium and (2) coculturing stem cells with cardiomyocytes in cell-contact modes. It has been found that stem-cell contact with neighboring cardiomyocytes can induce stem-cell differentiation and functional coupling[2, 3]. Not only does a coculture system provide soluble factors (e.g., cytokines, growth factors, and hormones), it also presents contact-mediated factors including mechanical and electrical signals transmitted through cell-adherent junctions[4] and gap junctions[5], which are crucial for intercellular communication. Conventional in vitro-study models involve random cell shapes, which result in an undefined mode of cell-cell contact including multiple homotypic and heterotypic contacts among the interacting cells. Therefore, conventional cell-culture models cannot provide identical and well-controlled in vitro microenvironments to systematically study the effects of cell-cell contact on stem cell-cardiomyocyte interactions[6]. The importance of cell-cell contact for stem-cell functional coupling with cardiomyocytes has not been elucidated due to insufficient control of the cell-contact mode of individual cells.

Biochips with well-defined cell arrangements have been developed for isolating and analyzing large quantities of individual cells in identical and controlled environments, which allow assessment of contact-mediated cell-cell interaction in a dynamic and high-throughput fashion. To create these biochips, microfabrication techniques have been widely used due to their advantages of confining cellular morphology, controlling or mimicking physiological microenvironment, improving culture efficiency, and achieving reproducible cultures[7–10]. With controlled microenvironments made by microfabrication techniques, it is possible to create biochips to promote or prevent cellular contact between individual stem cells and cardiomyocytes and allow for high-throughput screening of the behavior of single cells under identical microenvironments. However, the conventional microfabrication-based biochips achieved by trapping individual cells from a massive cell flow for cell seeding cannot provide single cell-based heterotypic micropatterning with high spatial and temporal resolution. To address this problem, the laser-guidance technique has been developed to specifically select individual cells and precisely place them onto biochips with high spatial resolution. The laser-guidance technique utilizes optical forces to radially trap a cell in the beam axis and axially guide it to a target surface. We developed a laser-guided cell-micropatterning system to achieve high-speed, heterotypic single-cell micropatterning with a microinjection mechanism and an on-stage incubator for long-term cell culturing during and after cell micropatterning[11].

In this study, two types of biochips were created to evaluate the electrical-property changes of individual rat mesenchymal stem cells (rMSCs) regulated by cardiomyocytes under identical, highly controlled microenvironments. Each type of biochip was microfabricated with a microenvironment in which individual rMSCs and cardiomyocytes were laser-patterned to interact with or without cellular contact. The changes in rMSC electrophysiological properties in the two types of biochips were compared at different time points, and the effect of cellular contact on the cardiogenic regulation of stem-cell electrical properties was systematically assessed.

## Materials and methods

### Cell handling

Cardiomyocytes were isolated and collected from three-day-old neonatal rats using a two-day protocol. After dissection, the ventricular portions of neonatal-rat hearts were collected and minced in Moscona's Saline. The heart tissue was transferred into 50 mL Dulbecco's Phosphate Buffered Saline (DPBS) with 4 mg trypsin and 50 mg neutral protease and stored overnight in a 4 °C refrigerator. The next day, the heart tissue was transferred into 50 mL Kreb's Ringers Bicarbonate Buffer (KRB) with 10 mg Collagenase type I and 30 mg Collagenase type II and then shaken in a water bath at 50 RPM for 1 hour. The cell suspension was washed twice using a cardiomyocyte culture medium (high glucose Dulbecco's Modified Eagle's Medium (DMEM) supplemented with 20% fetal bovine serum (FBS) and 1% penicillin streptomycin[12]) to remove the enzyme residue. Our experiments with various concentrations of FBS (5–20%) demonstrated that 20% FBS promoted healthy cell culture inside microwells with 40–60 μm depths. The isolated cells were transferred into a 150 $cm^2$ flask for preattachment to remove the cardiac fibroblasts. After two hours, the unattached cardiomyocytes were collected for subsequent use. According to a previous characterization[13], our isolation protocol yields approximately 95% cardiomyocytes. Because of the difference in size between cardiomyocytes and other non-myocyte cells, we can select and deposit only cardiomyocytes into the microwells during the laser-patterning procedure.

Commercial rat mesenchymal stem cells from bone marrow (rMSCs) were purchased from ScienCell™ research laboratories (California, USA). Before the shipment, rMSCs were characterized by ScienCell™ using the immunofluorescent method with antibodies to CD73, CD90, CD105, and oil red staining after adipocyte differentiation. The rMSCs were cultured using mesenchymal stem cell medium (MSCM) from the same company and used for laser-patterning before the fifth passage. The cardiomyocyte culture medium was used as the coculture medium for the biochips during and after the laser-patterning procedure.

The cellular morphology of cardiomyocytes and rMSCs in our random coculture was examined by immunostaining (shown in Figure 1). The culture was fixed at room temperature in 4% paraformaldehyde (10 min), 0.1% Triton X-100 (15 min), and blocked by 2% bovine serum albumin (BSA) and 4% serum. Then the cells were labeled by antibodies: mouse anti-α-actinin (A7811, Sigma-Aldrich, Missouri, USA) followed by donkey anti-mouse IgG-FITC as the secondary antibody and mouse anti-CD90 (sc-73163, Santa Cruz Biotechnology Inc., California, USA) with goat anti-mouse IgG-TR as the secondary antibody.

All experiments that involve animal use were performed in compliance with the relevant laws and institutional guidelines. These experiments have been approved by Clemson University's Institutional Animal Care and Use Committee through protocol AUP2010-032.

### Biochip fabrication

Two types of biochips were designed to study the role of cellular contact on cardiogenic regulation of stem-cell electrical properties: one with a contact-promotive microenvironment and the other with a contact-preventive microenvironment. The microenvironment was a microwell containing one stem cell and one cardiomyocyte. For each type of biochip, identical 9 × 9 microwells were created by attaching an elastomeric membrane with through holes onto a glass coverslip. The microwell for the contact-promotive biochip was designed as a rectangle (50 μm long and 25 μm wide), which confined the cell bodies of two cells to form physical contact. The microwell for the contact-preventive biochip was designed in a dumbbell shape with two circles (30 μm in diameter) connected by one channel (30 μm in

length and 20 μm in width). One rMSC and one cardiomyocyte were laser-patterned into the two circles separately. The curve between the circle and the channel prevented a cell from contacting the cell on the other side. The depth of the microwell was controlled at 40 μm, which restricted the cells inside the microwells and allowed micropipettes to reach the cell during patch-clamp experiments. The distance between two neighboring microwells was 200 μm.

Elastomeric membranes were microfabricated using polydimethylsiloxane (PDMS) with the standard lithographic procedure. The biochips were assembled by attaching the membranes to the glass coverslips and heating at 50 °C for 2 hours to create a permanent bond. Before being used, the biochips were cleaned, sterilized, and activated by oxygen plasma. Immediately following the plasma treatment, the biochips were coated with fibronectin to improve cell attachment and biocompatibility on the underlying glass substrate. The biochips were placed inside cell-deposition chambers, one biochip for each chamber, where individual stem cells and cardiomyocytes would be laser-patterned onto the biochip's microwells.

### Laser-guided cell micropatterning

The laser-guided cell micropatterning technique enabled accurate placement of individual rMSCs and cardiomyocytes onto the biochips. This unique technique[14] was critical to studying the regulation process of rMSC electrical properties at different time points. The details of the system design are discussed in our previous paper[15]. A typical cell-micropatterning procedure began with preparation of the biochip (i.e., a patterning substrate with a matrix of microwells) and the cell suspension. A 35 mm petri dish containing a biochip was sealed inside the cell-deposition chamber. The chamber was mounted on a 3-axis motorized translational stage, which was controlled to move relative to the laser beam and the imaging system. The imaging system's field-of-view was adjusted to the guidance region of the laser beam at the center of the imaging system's monitor screen. This allowed high-speed cell manipulation in three dimensions and continuous image tracing. A cell suspension with a concentration of 30,000 cells/mL was loaded into a 50 μl microsyringe and injected through a hollow fiber into the media-filled deposition chamber. The cell feed ratio was optimized for single-cell flow by adjusting the volume (50 nL) and speed (25 nL/s) of the microinjection. Once the cell was captured by the laser, the cell was guided to the destination (a microwell) by moving the chamber in three dimensions. To create a heterotypic cell pair, one cardiomyocyte was first laser-patterned into the left side of one microwell on the biochip, and then one rMSC was patterned into the right side of the microwell containing the cardiomyocyte. The orientation of the microwell can be determined by the triangular features established outside the central region, and thus rMSCs could be distinguished from cardiomyocytes in the following experiments.

### Patch clamp experiment

To study the cardiogenic regulation of rMSC electrical properties in the biochip-based assay, patch-clamp experiments were conducted on the cells inside the microwells from Day 1 to Day 5. Borosilicate glass electrodes were pulled with a Brown-Flaming puller (P-97, Sutter Instrument Co., California, USA) to achieve a tip resistance of 3–4 MΩ when the tip was filled with pipette solution. The pipette solution contained 140 mM K-gluconate, 1 mM EGTA, 2 mM $MgCl_2$, 2 mM $Na_2ATP$, and 10 mM HEPES (pH 7.2, 330 mOsm). The bath solution contained 139 mM NaCl, 3 mM KCl, 17 mM $NaHCO_3$, 12 mM Glucose, 3 mM $CaCl_2$, 1 mM $MgCl_2$, and 10 mM HEPES (pH 7.2, 330 mOsm). After establishing the whole-cell-patch configuration, the membrane potential was held at −70 mV with an addition of 90 mV voltage pulse, and current signals were recorded.

The patch clamp experiments were conducted using a computer-controlled current/voltage clamp (Multichannel 700A, Axon Instruments Co., California, USA) and a 16-bit data acquisition system (Digidata 1322A, Axon Instruments Co., California, USA) with slowly circulated media held at 37°C. Typically, it took less than 6 minutes to patch a cell and record the inward currents with voltage clamps. Each biochip had 81 cell pairs, but only viable cell pairs under good visual conditions were clamped. On average, approximately 10 pairs were studied for each biochip.

### Connexin 43 staining

The cells in the contact-promotive biochips were stained for connexin 43 on Day 5. The cells were fixed and blocked in 4% paraformaldehyde (10 min), 0.1% Triton X-100 (15 min), and 2% bovine serum albumin (BSA) with 4% goat serum, respectively. Next, the cells were labeled with a primary antibody, rabbit anti-Cx43 (C6219, Sigma-Aldrich, Missouri, USA), at a dilution of 1: 400 in 1× PBS at 4 °C overnight. Excess primary antibody was removed by a triple wash in PBS, and the cells were stained with Cy3-conjugated anti-rabbit IgG at dilution of 1: 100 in PBS at room temperature for 2 hours. After three washes with PBS to remove the secondary antibody, the slides were prepared with ProLong® antifade kit mounting medium with DAPI staining (Invitrogen Inc., New York, USA).

Immunostained cells were imaged using a confocal fluorescent microscope (Eclipse Ti, Nikon, Tokyo, Japan) with a 40X oil-immersed objective, a high sensitivity quantitative monochrome camera (CoolSnap HQ$^2$, Photometrics, Arizona, USA), and the Nikon imaging software (for image acquisition only). The image was obtained for each microwell with an exposure time of 400 ms and was not processed with image processing software. The nonspecific control groups (one group without primary antibodies and one group without secondary antibodies) were conducted simultaneously with the experimental group. Junction formation between contacted cells was determined through imaging data on connexin-43 expression: When the fluorescence image of connexin-43 expression features a thin line along the border of two contact cells as opposed to a diffusive distribution, junctional connection would be counted.

### Reverse transcription PCR

To further study the cardiogenic regulation of stem-cell electrical properties, the expression of cardiac-specific genes on rMSCs was analyzed by reverse transcription PCR (RT-PCR) in contact-promotive and contact-preventive random culture models. GATA4 and Nkx2.5 are transcriptional factors that are expressed in cardiomyocytes during early development, and ANP is a hormone secreted by cardiomyocytes[16]. Three genes were examined to determine the early differentiation of stem cells into a cardiac lineage. Cardiomyocyte-specific sodium (SCN1A and SCN 3A) and calcium channels (CACNA1C) were examined to determine the change in stem-cell electrophysiological properties[17].

The rMSCs prepared for the contact-promotive random culture model were labeled by DiI (Vybrant Multicolor Cell-Labeling Kit, Invitrogen Inc., New York, USA) and randomly cocultured with cardiomyocytes in a 25 cm$^2$ flask with an initial rMSC-cardiomyocyte ratio of 1: 40. The rMSCs were sorted on Day 6 using Cytopeia Influx flow cytometry. The rMSCs prepared for the contact-preventive random culture model were cultured for 6 days with the conditioned medium from a Day-3 cardiomyocyte culture. The RT-PCR-quantified RNA obtained from an rMSC culture was used as a control group. The total RNA was extracted using RNAeasy™ Mini kit (Qiagene Inc., Duesseldorf, Germany) and reverse transcribed into cDNA using SuperScript™ III First-strand Synthesis System (Invitrogen Inc., New York, USA). The sequences of rat oligonucleotide primers used in this RT-PCR

analysis are listed in Table 1. The relative quantification of gene expression by real-time RT-PCR in a sample was determined by comparing the target-amplified product against GAPDH within the same sample. The cycle threshold (Ct) was determined, and relative expression of cardiac-specific genes on rMSCs was analyzed using $2^{-\Delta\Delta Ct}$ method.

### Statistical analysis

The percentage of the cell pairs with the characteristic of interest (e.g., junctional connexin-43 expression, inward current formation, etc.) was calculated by equation (1) for each biochip (with 81 cell pairs). For each contact mode, 20 identical biochips were analyzed to collect statistical data, which were expressed as means ± SD. Statistical comparisons of data between two groups were performed using student's t-test: $p < 0.05$ was considered statistically significant.

$$\text{Percentage of characteristic} = \frac{\text{Number of cell pairs with this characteristics on one biochip}}{\text{Total number of viable cell pairs on the biochip}} \times 100\% \quad (1)$$

## Results and Discussions

### Cell pairs in microwells

The biochips with heterotypic cells were created by laser-patterning rMSCs and cardiomyocytes into the contact-promotive/preventive microwells, shown in Figure 2(a, b). The cardiomyocytes were on the left side of each microwell, and rMSCs were on the right side. Homotypic biochips that were created at the same time served as positive (two cardiomyocytes in one microwell) and negative (two rMSCs in one microwell) controls. Not all of the cell pairs survived after one day of culture; the round-shape cells inside the microwells were considered to be dead cells as shown in Figure 2(c). Such nonsurviving cell pairs were not counted in our further statistical studies. The viability ratio of cell pairs varied among the different types of biochips (contact-promotive and preventive) and different cell pairs (homotypic and heterotypic), but the average viability ratio was approximately 50%. In our previous research on patterning cells onto a glass coverslip, the viability of cells with the laser-patterning procedure did not show a significant difference from the cells without patterning[18]. The significant reduction in cell viability suggested that the limited geometric space and cell-cell connections inside a microwell might obstruct the exchange of nutrients and metabolic waste and thus cause lower cell viability compared to conventional cell cultures. Cell proliferation in the biochips was not observed during the experimental period, but spontaneous cardiomyocyte beating in the biochips after two-day culture was always observed.

In the contact-promotive biochips, 96 ± 5.2% of the viable heterotypic cell pairs filled the entire microwell and formed broad contact on their cell membranes as shown in Figure 2(d). The remaining pairs did not contact each other as shown in Figure 2(e). They were used as a contact-preventive model during the study of electrical coupling. In the contact-preventive biochip, 67 ± 6.6% of the viable heterotypic cell pairs did not contact each other. The noncontact cells stayed within their own side of the dumbbell-shape microwell (attached to the wall as shown in Figure 2(f)) and communicated with the other cell in the microwell only through soluble factors. The cardiomyocytes in the biochips were further confirmed by the immunostaining of α-actinin, which was absent on rMSCs, shown in Figure 3.

### Connexin 43 staining

Gap-junction channels are composed of connexins, a group of junctional proteins; connexin 43 is the most abundant one in the heart. In cardiac tissue, neighboring cardiomyocytes are

connected with gap junctions that provide electrical coupling with or without rectifying properties to propagate action potentials from one cell to another. Therefore, it was crucial to determine, through the assessment of the expression of connexin 43 in our biochips, the possible involvement of gap junctions in cardiogenic regulation of rMSC electrical properties. In the contact-promotive biochips, 84 ± 3.9% of the heterotypic cell pairs were observed with connexin 43 expression, among which 28 ± 6.5% exhibited junctional connexin 43 distribution at their contact area as shown in Figure 4(a, b). However, the others exhibited only diffuse connexin 43 distribution throughout the cell bodies as shown in Figure 4(c, d). In the contact-preventive biochips, only 59 ± 4.8% of surviving heterotypic cell pairs were found to express connexin 43, and the amount was small as shown in Figure 4(e, f). These connexin 43-staining data indicates that not only did cellular contact upregulate connexin 43 expression in rMSCs, it also relocated connexin 43 from the entire cell body to the contact area for rMSC-cardiomyocyte intercellular communication and electrical coupling. Gap-junction formation would provide rapid ion transfer, which might be one of the electrical signals that regulate stem-cell electrical properties towards cardiac electrophysiology.

## Electrophysiological regulation of rMSCs in microwells

Functional coupling between rMSCs and cardiomyocytes requires that rMSCs exhibit cardiac-like electrophysiology to invoke the action potential. Inward currents associated with the action potential are essential to the excitation and contraction of cardiomyocytes. Therefore, the appearance of inward currents is considered a specific indication for cardiogenic regulation of rMSC electrical properties. For the contact-promotive biochips, inward currents on the homotypic cardiomyocyte pairs (positive controls) reached about −2,000 pA as shown in Figure 5(a), but no inward current was recorded on the homotypic rMSC pairs that served as the negative controls. Inward currents on the heterotypic cell pairs are shown in Table 2. Both the percentage of rMSCs that exhibited inward currents and the magnitude of the inward currents increased with days in coculture. However, for the contact-preventive biochips, no inward current was recorded on the rMSCs in heterotypic cell pairs even on Day 5.

The inward current of a cardiomyocyte arose as soon as the voltage was clamped on the cell membrane; however, if an inward current obtained by patching a stem cell was from the contacted cardiomyocyte passively, there would be a time delay (more than 30 ms) between the leading edge of the inward current and the voltage clamp[19]. In our results, the time delay was around 10 ms, which was comparable to the time delay on the cardiomyocytes. This suggests that the inward currents recorded in our experiments came directly from the stem cells. The results suggests that cardiomyocytes could not regulate rMSC electrical properties without cellular contact with the rMSC, and contact with cardiomyocytes allowed rMSCs to gradually acquire electrophysiological properties that resembled the cardiac phenotype.

## Cardiac-specific gene expression

To explore the molecular mechanisms of electrical-property regulation in the contact-promotive biochips for determining the correlation between the regulation and the cardiogenic differentiation of rMSCs, cells from those prepared for the microwell assays were used simultaneously to produce three conventional cell-culture models: a contact-promotive random culture model, a contact-preventive random culture model, and a control model. The changes in cardiac-specific gene expression on rMSCs were compared among these three groups as shown in Figure 6. GATA4, Nkx2.5, and ANP genes were significantly upregulated in the noncontact groups relative to the control groups (1 fold). The upregulation of these gene expressions was higher in the contact-promotive coculture than in the noncontact group. This suggested that even with soluble chemical signals only,

the rMSCs could exhibit some cardiac genotypes expressed by the cardiomyocyte in a developmental heart. The sodium-channel genes (SCN1A and SCN3A) were not found in the noncontact groups, but small amounts were detected in the contact groups. However, the gene for L-type calcium channel (CACNA1C) was significantly upregulated in the contact groups, which could be a possible molecular basis for the inward currents recorded on the rMSCs in contact-promotive microwells. Small changes in calcium-channel gene expression were also detected in the noncontact groups. Since no inward current was recorded on rMSCs in contact-preventive microwells, there might be immature and dysfunctional calcium-channel proteins located inside the rMSC cytoplasm or cell membrane. After contact with cardiomyocytes, the calcium ion channels showed progressive stimulation and enhancement to functionally pump calcium ions into the cells and contribute to the inward current.

## Limitations

Smaller than a contact-preventive microwell, the volume of a contact-promotive microwell may cause a high local concentration of paracrine factors released from the adjacent cardiomyocyte. In addition, because microwell shape and curvature differ between contact-promotive and -preventive biochips, cell shape, spread, and attachment differ, and these may alter cell behavior. Our preliminary data obtained from microwells of different shapes, including a long-slot shape (30 μm in width and 200 μm in length) and circular microwells of different sizes (30, 50, and 70 μm in diameter), demonstrated (not shown in this paper) that cellular-contact status (contact or noncontact) is the dominant effect on cardiogenic regulation of stem-cell electrical properties. Because we have not systematically investigated effects of microwell shape and size on the stem cell's differentiation, we currently cannot draw any conclusion regarding potential effects.

Another limitation of this study is the use of neonatal cardiomyocytes, which exhibit uniform gap junctional distribution rather than the polar distribution characteristic of adult cardiomyocytes. Although heterotypic junctions and cardiogenic regulation from the neonatal cardiomyocytes in the cell pairs may differ from those seen in anisotropic adult heart tissue, it is important to note that cardiomyocytes in the infarct border zone also exhibit a uniform, neonatal-like distribution of gap junctions[20]. Conceivably, the interactions described in the cell pairs in this study may resemble cellular interactions in the border zone and prove to be highly relevant for the function of the infarcted heart and for the success and safety of cell implantation therapies.

## Conclusions

In conclusion, using laser-guided cell-micropatterning and microfabrication techniques, we created two types of biochips, with either contact-promotive or -preventive microenvironments, to systematically study the importance of cellular contact on the regulation of stem-cell electrical properties. The results from immunocytostaining, electrophysiology, and RT-PCR highlighted the ability of rMSCs to increase their electrical compatibility with host cardiomyocytes in a contact-promotive microenvironment. Control of their coupling microenvironment may eventually lead to the ability to guide the functional integration of stem cells inside the heart and promote the design of safe and efficient cardiac-cell therapies.

## Acknowledgments

This work has been partially supported by NIH (SC COBRE P20RR021949 and Career Award 1k25hl088262-04); NSF (MRI, CBET-0923311 and SC EPSCoR RII EPS-0903795 through SC GEAR program); and Guangdong Provincial Department of Science and Technology, China (2011B050400011). JXY and BZG would also like to

acknowledge the support from the grant established by the State Key Laboratory of Precision Measuring Technology and Instruments (Tianjin University).

## References


1. Joggerst SJ, Hatzopoulos AK. Stem cell therapy for cardiac repair: benefits and barriers. Expert Rev Mol Med. 2009; 11:e20. [PubMed: 19586557]
2. Fukuhara S, Tomita S, Yamashiro S, Morisaki T, Yutani C, Kitamura S, Nakatani T. Direct cell-cell interaction of cardiomyocytes is key for bone marrow stromal cells to go into cardiac lineage in vitro. J Thorac Cardiovasc Surg. 2003; 125(6):1470–80. [PubMed: 12830069]
3. Yoon J, Shim WJ, Ro YM, Lim DS. Transdifferentiation of mesenchymal stem cells into cardiomyocytes by direct cell-to-cell contact with neonatal cardiomyocyte but not adult cardiomyocytes. Ann Hematol. 2005; 84(11):715–21. [PubMed: 16096830]
4. Gumbiner BM. Regulation of cadherin-mediated adhesion in morphogenesis. Nat Rev Mol Cell Biol. 2005; 6(8):622–34. [PubMed: 16025097]
5. Wei CJ, Xu X, Lo CW. Connexins and cell signaling in development and disease. Annu Rev Cell Dev Biol. 2004; 20:811–38. [PubMed: 15473861]
6. Pedrotty DM, Klinger RY, Badie N, Hinds S, Kardashian A, Bursac N. Structural coupling of cardiomyocytes and noncardiomyocytes: quantitative comparisons using a novel micropatterned cell pair assay. Am J Physiol Heart Circ Physiol. 2008; 295(1):H390–400. [PubMed: 18502901]
7. Revzin A, Sekine K, Sin A, Tompkins RG, Toner M. Development of a microfabricated cytometry platform for characterization and sorting of individual leukocytes. Lab Chip. 2005; 5(1):30–7. [PubMed: 15616737]
8. Di Carlo D, Wu LY, Lee LP. Dynamic single cell culture array. Lab Chip. 2006; 6(11):1445–9. [PubMed: 17066168]
9. Thery M, Racine V, Pepin A, Piel M, Chen Y, Sibarita JB, Bornens M. The extracellular matrix guides the orientation of the cell division axis. Nat Cell Biol. 2005; 7(10):947–53. [PubMed: 16179950]
10. Bray MA, Sheehy SP, Parker KK. Sarcomere alignment is regulated by myocyte shape. Cell Motil Cytoskeleton. 2008; 65(8):641–51. [PubMed: 18561184]
11. Pirlo RK, Sweeney AJ, Ringeisen BR, Kindy M, Gao BZ. Biochip/laser cell deposition system to assess polarized axonal growth from single neurons and neuronglia pairs in microchannels with novel asymmetrical geometries. Biomicrofluidics. 2011; 5(1):13408. [PubMed: 21522498]
12. Xu M, Wani M, Dai YS, Wang J, Yan M, Ayub A, Ashraf M. Differentiation of bone marrow stromal cells into the cardiac phenotype requires intercellular communication with myocytes. Circulation. 2004; 110(17):2658–65. [PubMed: 15492307]
13. Borg KT, Burgess W, Terracio L, Borg TK. Expression of metalloproteases by cardiac myocytes and fibroblasts in vitro. Cardiovasc Pathol. 1997; 6(5):261–9.
14. Odde DJ, Renn MJ. Laser-guided direct writing for applications in biotechnology. Trends Biotechnol. 1999; 17(10):385–9. [PubMed: 10481169]
15. Pirlo RK, Ma Z, Sweeney A, Liu H, Yun JX, Peng X, Yuan X, Guo GX, Gao BZ. Laser-guided cell micropatterning system. Rev Sci Instrum. 2011; 82(1):013708. [PubMed: 21280838]
16. Fukuda K. Development of regenerative cardiomyocytes from mesenchymal stem cells for cardiovascular tissue engineering. Artif Organs. 2001; 25(3):187–93. [PubMed: 11284885]
17. Li GR, Deng XL, Sun H, Chung SS, Tse HF, Lau CP. Ion channels in mesenchymal stem cells from rat bone marrow. Stem Cells. 2006; 24(6):1519–28. [PubMed: 16484345]
18. Rosenbalm TN, Owens R, Bakken D, Gao BZ. Cell viability test after laser guidance. Proc SPIE. 2006; 6084:299–306.
19. Tufan H, Cleemann L, Sussman M, Morad M. $Ca^{2+}$ transients in Pim-1 transfected cardiac stem cells co-cultured with rat neonatal cardiomyocytes. Biophys J. 2010; 98(3):134a.
20. Peter NS, Wit AL. Gap junction remodeling in infarction: does it play a role in arrhythmogenesis? J Cardiovasc Electrophysiol. 2000; 11:488–490. [PubMed: 10809506]

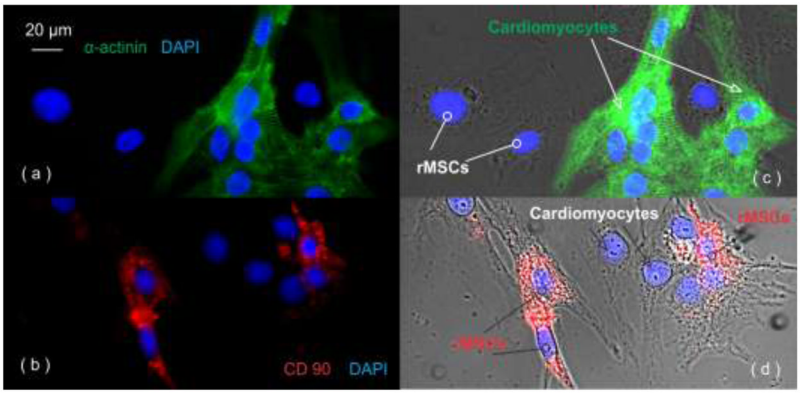


**Figure 1.**
Confocal images of cardiomyocytes and rMSCs in our random coculture system: (a) myocyte-specific staining of α-actinin and (c) α-actinin staining overlapped with bright field (α-actinin positive (green): cardiomyocytes; α-actinin negative: rMSCs); (b) rMSC specific staining of CD90 and (d) CD90 staining overlaped with bright field (CD90 positive (red): rMSCs; CD90 negative: cardiomyocytes); the cell nuclei stained by DAPI (blue).

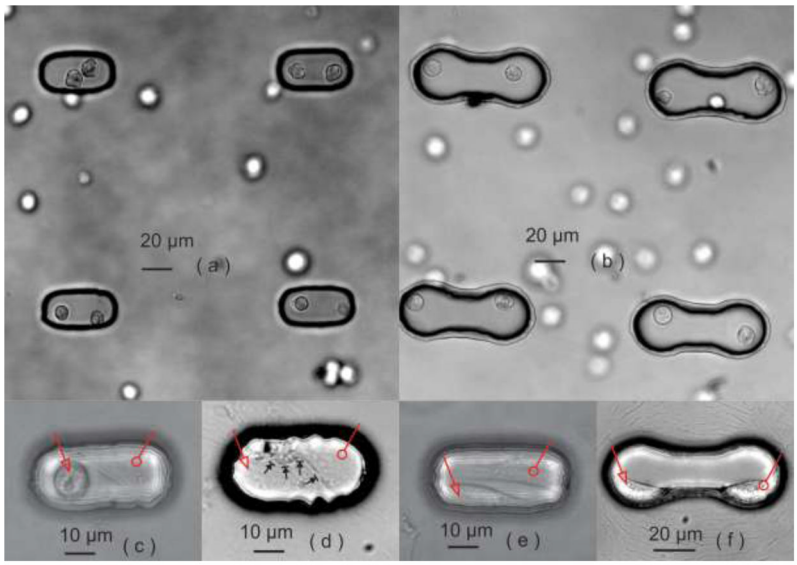


**Figure 2.**
Biochips with (a) a contact-promotive microenvironment and (b) a contact-preventive microenvironment captured immediately after laser micropatterning. (c) Nonsurviving heterotypic cell pairs in contact-promotive biochips. (d) Most surviving heterotypic cell pairs formed broad contact on their cell membranes in the contact-promotive cell biochip (black arrows), (e) but some did not form contact with each other. (f) The cardiomyocytes and rMSCs in the contact-preventive biochips remained separated, one on each side of a microwell. In figures (c–f), the hollow arrow points to a cardiomyocyte and the hollow circle points to an rMSC.

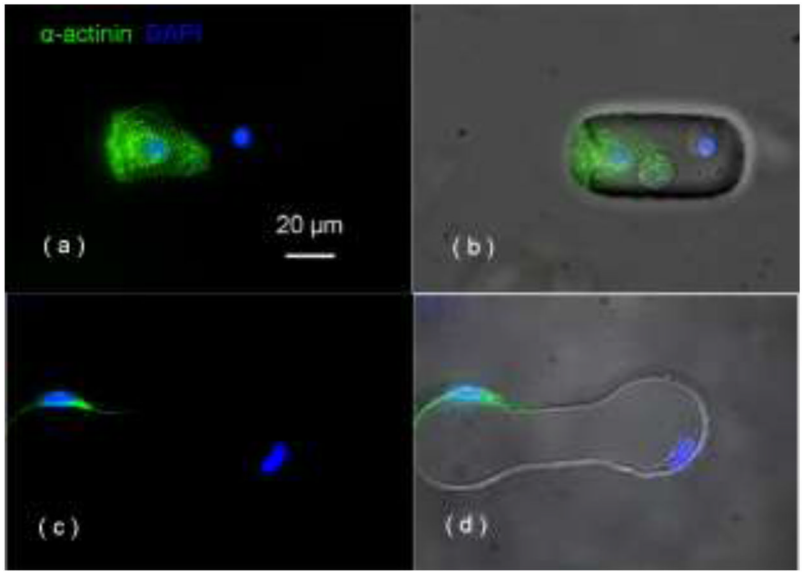


**Figure 3.**
positive α-actinin staining indicates the cardiomyocyte, negative staining indicates the rMSC in (a, b) the contact-promotive biochip and (c, d) the contact-preventive biochip; the cell nuclei was stained by DAPI (blue).

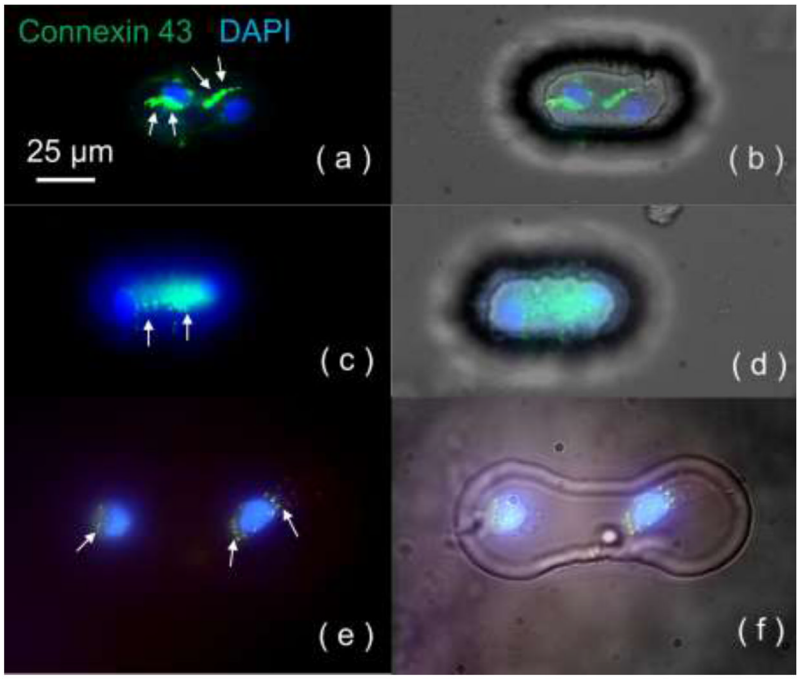


**Figure 4.**
Connexin 43 staining for contact-promotive/preventive biochips. The DAPI staining (blue) on the nucleus indicates two cells in one microwell, and Cy3 staining (green) indicates connexin 43 expression. (a, b) Junctional connexin 43 distribution at the cell-contact area was found in contact-promotive biochips; (c, d) Diffusive connexin 43 was expressed throughout the cell bodies in contact-promotive biochips. (e, f) In the contact-preventive biochips, portions of surviving heterotypic cell pairs were found to have diffusive connexin 43 expression. White arrows indicated the location of connexin 43.

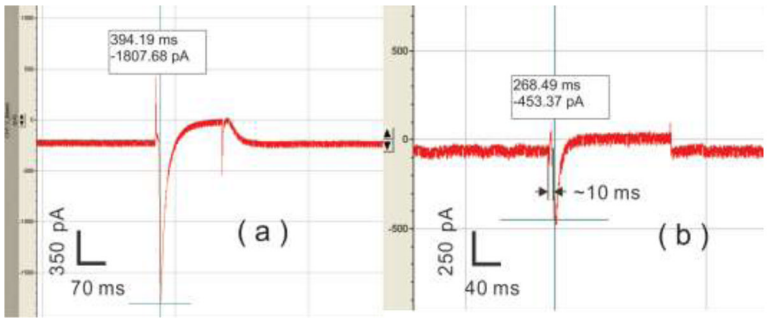


**Figure 5.**
Typical inward currents recorded on Day 5 from (a) the homotypic cardiomyocyte pairs in positive-control biochips and (b) rMSCs of heterotypic cell pairs in contact-promotive biochips.

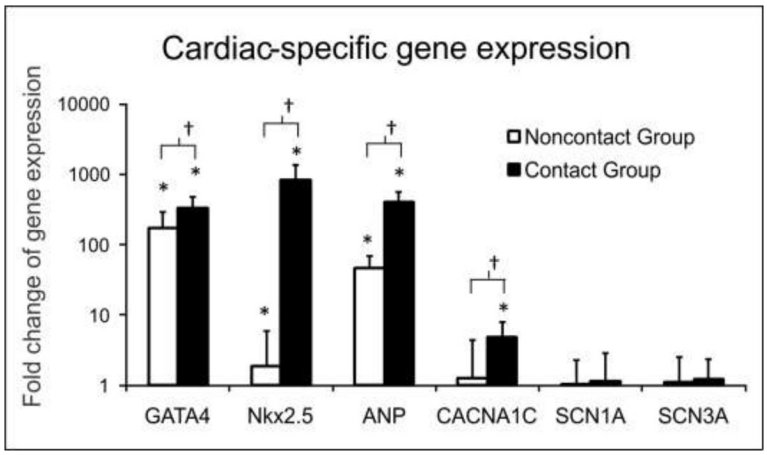


**Figure 6.**
RT-PCR analysis of cardiac-specific gene expression of the rMSCs from contact and noncontact groups relative to that of an rMSC control group (1 fold). *The gene expressed was significantly upregulated compared to the control group ($p < 0.005$); †The gene expressed in contact groups was significantly upregulated compared to noncontact groups ($p < 0.01$).

**Table 1**

The sequences of primers for cardiac specific genes and GAPDH reference

| Genes | Sequences |
|---|---|
| GATA4 (transcriptional factor) | F 5′-GCAGCAGCAGCAGTGAAGAG-3′<br>R 5′-GCACTGGATGGATGGAGGAC-3′ |
| Nkx2.5 (transcriptional factor) | F 5′-TGCTCTCCTGCTTTCCCAAC-3′<br>R 5′-GTCTCGGCTTTGTCCAGCTC-3′ |
| ANP (atrial nutriurentic peptide) | F 5′-AAGCAAACTGAGGGCTCTGC-3′<br>R 5′-TCGAGCAGATTTGGCTGTTAT-3′ |
| CACNA1C (L-calcium channel) | F 5′-AGGAGTTTCCTTCGCTCTGC-3′<br>R 5′-AAGGGCAAGGCTGTCTTCTG-3′ |
| SCN1A (sodium channel) | F 5′-GATGCTGTCAGTGCATGTCG-3′<br>R 5′-TCTGCTGAACGGTTTCCTTG-3′ |
| SCN3A (sodium channel) | F 5′-GGTCCATGCCAAACTGACTG-3′<br>R 5′-GCTGGTAATGGAAGCAGCAAC-3′ |
| GAPDH (reference) | F 5′-GAGACAGCCGCATCTTCTTG-3′<br>R 5′-GGTAACCAGGCGTCCGATAC-3′ |

**Table 2**

Inward current measurement in the biochips (mean ± SD, n = 20 for each group)

| | Day 1 | Day 2 | Day 3 | Day 4 | Day 5 |
|---|---|---|---|---|---|
| rMSCs | 0% | 13 ± 6.8% | 21 ± 8.4% | 30 ± 7.9% | 28 ± 8.2% |
| (heterotypic/contact-promotive) | 0 pA | −214 ± 62 pA | −350 ± 59 pA | −435 ± 77 pA | −422 ± 63 pA |
| rMSCs (homotypic/contact-promotive) | No inward current | | | | |
| rMSCs (heteroptypic/contact-preventive) | No inward current | | | | |
| Cardiomyocytes | 100% | | | | |
| (homotypic/contact-promotive) | −2,011 ± 177 pA | | | | |